REPORT DOCUMENTATION PAGE

Form Approved OMB NO. 0704-0188

1. REPORT DATE (DD-MM-YYYY)	2. REPORT TYPE	3. DATES COVERED (From - To)
15-12-2015	Final Report	2-Aug-2010 - 1-Aug-2013

4. TITLE AND SUBTITLE
Final Report: Research Area 4. Electronics. Bio-Inspired Radio-Frequency (RF) Direction Finding

5a. CONTRACT NUMBER
W911NF-10-1-0285

5b. GRANT NUMBER

5c. PROGRAM ELEMENT NUMBER
611102

6. AUTHORS
Hao Xin

5d. PROJECT NUMBER

5e. TASK NUMBER

5f. WORK UNIT NUMBER

7. PERFORMING ORGANIZATION NAMES AND ADDRESSES
University of Arizona
P.O. Box 210158, Rm 510

Tucson, AZ 85721 -0158

8. PERFORMING ORGANIZATION REPORT NUMBER

9. SPONSORING/MONITORING AGENCY NAME(S) AND ADDRESS (ES)
U.S. Army Research Office
P.O. Box 12211
Research Triangle Park, NC 27709-2211

10. SPONSOR/MONITOR'S ACRONYM(S)
ARO

11. SPONSOR/MONITOR'S REPORT NUMBER(S)
57268-EL.24

12. DISTRIBUTION AVAILIBILITY STATEMENT
Approved for Public Release; Distribution Unlimited

13. SUPPLEMENTARY NOTES
The views, opinions and/or findings contained in this report are those of the author(s) and should not contrued as an official Department of the Army position, policy or decision, unless so designated by other documentation.

14. ABSTRACT
This document is the final technical report for the "Biologically Inspired RF Direction Finding" project funded by the Army Research Office (ARO) under research agreement No. W911NF-1-01-0285. We have been investigating novel RF direction finding techniques inspired by human auditory system with the goal of achieving high performance and portable RF direction finding systems. We have studied improved two-antenna microwave passive direction finding systems inspired by human auditory system. By incorporating a head-like scatterer in between two antennas, additional magnitude information can be utilized to estimate the direction of arrival (DoA) of a

15. SUBJECT TERMS
Direction Finding, Biological Inspired

16. SECURITY CLASSIFICATION OF:			17. LIMITATION OF ABSTRACT	15. NUMBER OF PAGES	19a. NAME OF RESPONSIBLE PERSON
a. REPORT	b. ABSTRACT	c. THIS PAGE			Hao Xin
UU	UU	UU	UU		19b. TELEPHONE NUMBER 520-626-6941

Report Title

Final Report: Research Area 4. Electronics. Bio-Inspired Radio-Frequency (RF) Direction Finding

ABSTRACT

This document is the final technical report for the "Biologically Inspired RF Direction Finding" project funded by the Army Research Office (ARO) under research agreement No. W911NF-1-01-0285. We have been investigating novel RF direction finding techniques inspired by human auditory system with the goal of achieving high performance and portable RF direction finding systems. We have studied improved two-antenna microwave passive direction finding systems inspired by human auditory system. By incorporating a head-like scatterer in between two antennas, additional magnitude information can be utilized to estimate the direction of arrival (DoA) of a microwave signal, thus eliminating ambiguities associated with phase wrapping at high frequency, just like human ears. A new portable DF system design based on PIFA antennas that are well suited for wireless mobile applications has been completed and tested in laboratory environment. Furthermore, it has been demonstrated that this technique can be extended to 3-D direction finding (DF). In addition, better DoA sensitivity is demonstrated with the incorporation of high-permittivity scatterer due to the enhanced phase difference. A novel DoA technique for broadband microwave signals is also investigated. A single Ultra-Wide-Band (UWB) antenna, inspired by the sound source localization ability of human auditory system using just one ear (monaural localization), has been utilized. By exploiting the incident angle dependent frequency response of a wide-band antenna, the DoA of a broadband microwave signal can be estimated. DoA estimation accuracies are evaluated for various antennas and microwave signals under different signal-to-noise ratio (SNR) scenarios. Promising DoA performance of the proposed technique is demonstrated in both simulation and experiment. Another single antenna DF demonstration based on a leaky wave antenna has also been accomplished. In addition, a broadband passive direction finding system utilizing Luneburg lens has been investigated. Finally, a portable and reliable inventory localization system incorporating the distance (obtained from ultrasound) and direction information (obtained from previously described RF techniques) has been demonstrated. Detailed technical accomplishments are described in section II of this report.

Enter List of papers submitted or published that acknowledge ARO support from the start of the project to the date of this printing. List the papers, including journal references, in the following categories:

(a) Papers published in peer-reviewed journals (N/A for none)

Received Paper

TOTAL:

Number of Papers published in peer-reviewed journals:

(b) Papers published in non-peer-reviewed journals (N/A for none)

Received Paper

TOTAL:

Number of Papers published in non peer-reviewed journals:

(c) Presentations

Number of Presentations: 1.00

Non Peer-Reviewed Conference Proceeding publications (other than abstracts):

Received	Paper

TOTAL:

Number of Non Peer-Reviewed Conference Proceeding publications (other than abstracts):

Peer-Reviewed Conference Proceeding publications (other than abstracts):

Received		Paper
08/21/2012	10.00	Xiaoju Yu, Hao Xin. Direction of Arrival Estimation with Two Planar Inverted F Antennas and a Scatter, IEEE AP / URSI 2012. 07-JUL-12, . : ,
08/21/2012	14.00	Xiaoju Yu, Min Liang, Rafael Sabory-Garcia, Michael Gehm, Hao Xin. NOVEL BROADBAND DIRECTION OF ARRIVAL ESTIMATION USING LUNEBURG LENS, International Telemetering Conference. 22-OCT-12, . : ,
08/21/2012	12.00	Xiaoju Yu , Rafael Sabory Garcia , Min Liang , Weiren Ng, Michael Gehm, Hao Xin. Direction of arrival estimation using Luneburg lens, IEEE Microwave Symposium 2012. 18-JUN-12, . : ,
08/21/2012	11.00	Xiaoju Yu, Hao Xin. Direction of Arrival Estimation Utilizing Incident Angle Dependent Spectra, IEEE Microwave Symposium 2012. 18-JUN-12, . : ,
11/19/2015	15.00	xiaoju yu, hao xin. Radio-Frequency Direction Finding Inspired by Human Ears, Asian Pacific Conf. on Antennas and Propagation (APCAP). 26-JUL-14, . : ,
11/19/2015	19.00	Xiaoju Yu, Hao Xin. Direction of Arrival Estimation Improvement for Closely Spaced Electrically Small Antenna Array, International Telemetering Conference 2013. 21-DEC-13, . : ,
11/19/2015	18.00	Xiaoju Yu, Hao Xin. Direction of Arrival Estimation Enhancement for Closely Spaced Electrically Small Antenna Array, URSI 2014, Boulder Colorado. 06-JAN-14, . : ,
11/19/2015	17.00	Xiaoju Yu, Hao Xin. Direction of Arrival Estimation of Broadband Signal Using Single Antenna, International Telemetering Conference . 20-OCT-14, . : ,
11/19/2015	16.00	Xiaoju Yu, Hao Xin. Impact of Matching Networks on Direction Finding Performance Utilizing Two Closely Spaced Electrically Small Antennas, IEEE AP/URSI Symp., Memphis, July 2014.. 06-JUL-14, . : ,
11/29/2011	2.00	Hao Xin, Hao Xin. Conference Proceeding: Biological Inspired RF Direction Finding, Government Microcircuit Applications and Critical Technology Conference (GOMAC). 23-MAR-11, . : ,
11/29/2011	3.00	Rongguo Zhou, Hao Xin. A Novel Direction of Arrival Estimation Technique Using a Single UWB Antenna, IEEE Antennas and Propagation Symposium. 11-JUL-10, . : ,
11/29/2011	6.00	Xiaoju Yu, Hao Xin. 3-D Direction of Arrival Estimation with Two Antennas, International Telemetering Conference. 25-OCT-11, . : ,

TOTAL: 12

Number of Peer-Reviewed Conference Proceeding publications (other than abstracts):

(d) Manuscripts

Received		Paper
08/21/2012	9.00	Duixian Liu, Rongguo Zhou, Hao Xin. A Wideband Circularly Polarized Patch Antenna for 60 GHz Wireless Communications,, WIRELESS Engineering and Technology (03 2012)
08/21/2012	13.00	Xiaoju Yu , Rongguo Zhou , Hualiang Zhang, Hao Xin. A Microwave Direction of Arrival Estimation Technique Using a Single Antenna, IEEE Antennas and Propagaton Transactions (08 2012)
11/29/2011	1.00	Hualiang Zhang, Hao Xin, Rongguo Zhou. Improved Two-Antenna Direction Finding Inspired by Human Ears, IEEE Antennas and Propagaton Transactions (07 2011)
11/29/2011	7.00	Xiaoju Yu, Min Liang, Rafael Austrebert Sabory Garcia, Hao Xin. Ultra Wide Band Microwave Direction of Arrival Estimation Using Luneburg Lens, IEEE Antennas and Wireless Propagation Letters (11 2011)
11/29/2011	8.00	Xiaoju Yu, Rongguo Zhou, Hualiang Zhang, Hao Xin. A Microwave Direction of Arrival Estimation Technique Using a Single Antenna, IEEE Antennas and Propagaton Transactions (11 2011)
12/15/2015	20.00	Rongguo Zhou, Hualiang Zhang, Hao Xin, Xiaoju Yu. A Microwave Direction of Arrival Estimation Technique Using a Single Antenna, IEEE Antennas and Propagaton Transactions (09 2015)
12/15/2015	21.00	Xiaoju Yu, Hao Xin. Direction of Arrival Estimation Enhancement for Closely Spaced Electrically Small Antenna Array, IEEE AWPL (02 2016)
12/15/2015	22.00	Min Liang, Hao Xin, Xiaoju Yu. Ultra Wide Band Microwave Direction of Arrival Estimation Using Luneburg Lens, IEEE AWPL ( )
12/15/2015	23.00	Xiaoju Yu, Hao Xin. Portable Radio Frequency and Ultrasound Hybrid System for Inventory Localization, IEEE AWPL ( )
TOTAL:		**9**

Number of Manuscripts:

Books

Received Book

TOTAL:

Received Book Chapter

TOTAL:

Patents Submitted

H. Xin, and X. Yu, "RF and Ultrasound Hybrid System for Inventory Localization," Provisional application – UA14-026, Aug. 2013.

Patents Awarded

Awards

Second prize of graduate student paper competition, International Telemetering Conference (ITC), Oct., 2014

Second prize of graduate student paper competition, International Telemetering Conference (ITC), Oct., 2013

Graduate Students

NAME	PERCENT_SUPPORTED	Discipline
Rongguo Zhou	0.50	
Xiaoju Yu	0.50	
Min Liang	0.20	
FTE Equivalent:	**1.20**	
Total Number:	**3**	

Names of Post Doctorates

NAME	PERCENT_SUPPORTED
FTE Equivalent:	
Total Number:	

Names of Faculty Supported

NAME	PERCENT_SUPPORTED	National Academy Member
Hao Xin	0.15	
FTE Equivalent:	**0.15**	
Total Number:	**1**	

Names of Under Graduate students supported

NAME	PERCENT_SUPPORTED
FTE Equivalent:	
Total Number:	

Student Metrics

This section only applies to graduating undergraduates supported by this agreement in this reporting period

The number of undergraduates funded by this agreement who graduated during this period: .....

The number of undergraduates funded by this agreement who graduated during this period with a degree in science, mathematics, engineering, or technology fields:.....

The number of undergraduates funded by your agreement who graduated during this period and will continue to pursue a graduate or Ph.D. degree in science, mathematics, engineering, or technology fields:.....

Number of graduating undergraduates who achieved a 3.5 GPA to 4.0 (4.0 max scale):.....

Number of graduating undergraduates funded by a DoD funded Center of Excellence grant for Education, Research and Engineering:.....

The number of undergraduates funded by your agreement who graduated during this period and intend to work for the Department of Defense .....

The number of undergraduates funded by your agreement who graduated during this period and will receive scholarships or fellowships for further studies in science, mathematics, engineering or technology fields: .....

Names of Personnel receiving masters degrees

NAME
Rongguo Zhou
Total Number: **1**

Names of personnel receiving PHDs

NAME
Rongguo Zhou
Total Number: **1**

Names of other research staff

NAME	PERCENT_SUPPORTED
FTE Equivalent:	
Total Number:	

Sub Contractors (DD882)

Inventions (DD882)

Scientific Progress

See Attachment.

Technology Transfer

Final Technical Report
for Army Research Office (ARO) Research Agreement No. W911NF-1-01-0285
BIOLOGICALLY INSPIRED RADIO-FREQUENCY (RF) DIRECTION FINDING

Hao Xin, Professor
Electrical and Computer Engineering Department, and Physics Department
University of Arizona

Table of Contents

Abstract – This document is the final technical report for the "Biologically Inspired RF Direction Finding" project funded by the Army Research Office (ARO) under research agreement No. W911NF-1-01-0285. We have been investigating novel RF direction finding techniques inspired by human auditory system with the goal of achieving high performance and portable RF direction finding systems. We have studied improved two-antenna microwave passive direction finding systems inspired by human auditory system. By incorporating a head-like scatterer in between two antennas, additional magnitude information can be utilized to estimate the direction of arrival (DoA) of a microwave signal, thus eliminating ambiguities associated with phase wrapping at high frequency, just like human ears. A new portable DF system design based on PIFA antennas that are well suited for wireless mobile applications has been completed and tested in laboratory environment. Furthermore, it has been demonstrated that this technique can be extended to 3-D direction finding (DF). In addition, better DoA sensitivity is demonstrated with the incorporation of high-permittivity scatterer due to the enhanced phase difference. A novel DoA technique for broadband microwave signals is also investigated. A single Ultra-Wide-Band (UWB) antenna, inspired by the sound source localization ability of human auditory system using just one ear (monaural localization), has been utilized. By exploiting the incident angle dependent frequency response of a wide-band antenna, the DoA of a broadband microwave signal can be estimated. DoA estimation accuracies are evaluated for various antennas and microwave signals under different signal-to-noise ratio (SNR) scenarios. Promising DoA performance of the proposed technique is demonstrated in both simulation and experiment. Another single antenna DF demonstration based on a leaky wave antenna has also been accomplished. In addition, a broadband passive direction finding system utilizing Luneburg lens has been investigated. Finally, a portable and reliable inventory localization system incorporating the distance (obtained from ultrasound) and direction information (obtained from previously described RF techniques) has been demonstrated. Detailed technical accomplishments are described in section II of this report.

I. Statement of the Problem Studied

DoA estimation of an electromagnetic signal is important for many commercial and military applications including electronic warfare [1] and mobile communications [2]. Most attention has been paid on arrays consisting of a large number of antennas and sophisticated algorithms to achieve high degree of accuracy [1]. However, as the number of antenna elements increases, the power consumption, size and cost of the system increase as well, which would be impractical especially for portable and commercial applications. Therefore, accurate DoA estimation technique with reduced number of antennas is highly desirable.

Passive direction finding for microwave signal is very analogous to the direction finding of acoustic wave by human ears. Figure 1 illustrates the analogy between a microwave direction finding system and the human auditory system. The microwave antennas are similar to the pinnae, which are natural directional antennas for acoustic waves; the band-pass filters, amplifiers, mixers and detectors provide similar functions as the guiding and detecting parts of the human auditory system; and the signal processing components can be thought as the brain.

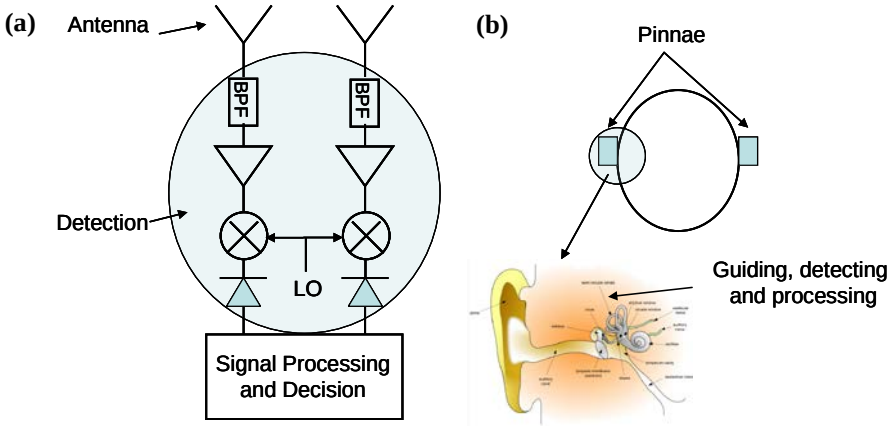

Figure 1. Comparison of a passive microwave direction finding system (a) and the human auditory system (b).

The remarkable localization (mainly in the azimuth plane) capabilities of human ears for both continuous waves (CW) and transient signals have long been recognized and studied quite extensively [3-8]. Many intriguing facts and phenomena were experimentally observed and underlying mechanisms were proposed and proved. As early as 1936, Stevens and Newman reported free space experimental data on localization of sound sources by human ears which revealed the two main mechanisms of binaural sound localization, one operating best at high frequency and the other at low frequency [6]. Later on, more studies in anechoic chambers confirmed the earlier results [7-8]. For most of the audible frequency range (20 Hz – 20 KHz), human ears have the amazing ability of estimating arrival angle with accuracy up to 1° without ambiguity under binaural (utilizing two ears) conditions.

For low frequency sound (f <1.5 – 3.0 KHz), the phase difference between the acoustic signals received by the two ears (referred to as the binaural case) serves as the most important cue. To avoid the phase ambiguity of multiples of 2π, the antenna elements should be spaced less than half a wavelength, $\lambda/2$. The front-back ambiguity is eliminated by the directivity of human ears (analogous to an antenna radiation pattern) [3]. For higher frequency sound (f > 3.0 KHz), the head can be thought as a low-pass filter. For most incident angles, one ear receives without the influence of the head while the other receives after the incident signal goes through (or around) the low-pass filter - human head, whose response function is incident angle dependent and can have an attenuation as much as 20 dB [5]. This effect is often referred to as the head-related-transfer function (HRTF), which leads to both a phase and a magnitude difference between the received signals at two ears. The combination of the phase (or time for transient signals) and amplitude information enables the human auditory system to have great localization capabilities for both low and high frequency ranges.

Both of the binaural mechanisms mentioned above have analogies or may be directly applied to microwave systems. The low-frequency phase difference method is widely used in microwave direction finding [1]. The high-frequency scheme utilizing an effective low-pass filter (the shadowing effect of human head) for azimuth-plane direction finding has been reported in [9][10]. By introducing a carefully designed scatterer in between two adjacent antennas, accurate direction finding without phase ambiguity for high frequency signals may be achieved. Furthermore, because of the spacing between the adjacent antenna elements can now be much larger than $\lambda/2$, the mutual coupling issue that is common to antenna array systems can be greatly reduced. In addition, 3-D (azimuth and elevation) direction finding technique is proposed by optimizing the scatter geometry and material parameters. Moreover, a new technique with advantage of compact size utilizing a high-permittivity scatterer in between two electrically small antennas to enhance directional sensitivity by enhancing their phase difference is demonstrated. The impact of the scatterer properties (i.e., shape, dielectric constant) on the directional sensitivity is studied. Then the DoA

performance of the system under various widely used matching networks such as self-conjugate match, Eigen-mode decoupling match and multi-port conjugate match is studied and analyzed.

Another amazing capability of the human auditory system is the monaural direction finding. Although not as accurate as the binaural (utilizing both ears) case, monaural direction finding is possible without head movement. This first seems to be intuitively unthinkable for a single stationary antenna. However, the monaural localization only works for broadband signals and the main mechanism has been identified to be the spectral alteration by the pinnae and head that provides cue for directions (similar to an incident angle sensitive "comb-line filter") [11, 12]. For example, as a simplified illustration shown in Figure 1, the received broadband signal by a single ear may have a notch response that is incident angle dependent. Therefore, monaural direction finding works only for broadband signals. Experimentally measured frequency dependent single ear head-related transfer functions for both azimuth and elevation planes can be found in [13]. By designing the frequency dependences of antenna pattern and guiding structure, this unique feature of human ear may be utilized for microwave applications such as direction finding for an ultra-wide-band (UWB) signal [14].

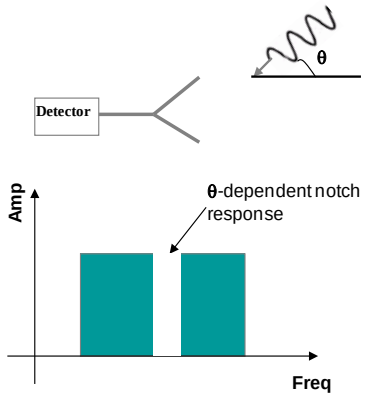

Figure 2. Simplified illustration of monaural direction finding of human auditory system: the received amplitude spectrum of an incoming broadband signal depends on the incident angle of the signal.

To investigate the broadband microwave direction finding technique, a previously demonstrated linear-polarized elliptical UWB (3.1 to 10.6 GHz) antenna [15] is used to investigate the single antenna direction finding technique [16], enabling DoA estimation using incident angle dependent received spectrum of a broadband signal. An improved UWB antenna with asymmetrical shape (D shape) is also designed and studied, demonstrating improved estimation accuracy due to the break of symmetry. Both UWB antennas are fabricated and their DoA performance is tested in an anechoic chamber using a horn antenna as the illuminator. The measured results confirm the feasibility of the proposed single antenna DoA technique. A microstrip leaky wave antenna (LWA) [17] is also studied for its main-beam-steering ability over the working frequency range. In other words, a LWA is able to function as a band pass filter with an arrival-angle-dependent center frequency, which is analogous to the incident-angle-dependent notch frequency response of human ears. Although the microstrip LWA has a relatively large size (usually several wavelengths because it is a travelling-wave antenna), the LWA is good for its simplicity in terms of both structure and feeding method.

The direction finding system using two monopoles with a lossy scatterer in between is relatively narrow banded because of the intrinsic antenna element property while the UWB single-antenna direction finding system can only detect broadband incident signals. Luneburg lens [4] based direction finding system is a good candidate to achieve a low cost, accurate and broadband direction finding system. A Luneburg lens has the characteristic that every point on the surface of the lens is the focal point of a plane wave incident from the opposite side as shown in Fig. 3. With a number of detectors mounted on the surface of a Luneburg lens, the DoA can be estimated by considering the received power distribution on all the

detectors. This novel direction finding system is advantageous in that it is really wide banded. In addition, the high gain property of a Luneburg lens leads to small correlation between received power distributions for different incident angles, thus high accuracy for the incident angle estimation can be achieved.

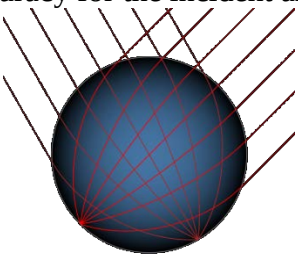

Figure 3. Optical path of plane waves incident on a Luneburg lens.

In practice, localization in addition to direction finding is often needed. For example, inventory localization of items such as a book, a laptop, a package, or even a sheep is highly desirable. GPSs are popular in outdoor real-time localization scenario [18]. However, the accuracy of a GPS may not be sufficient for inventory localization applications, especially in indoor cases. A novel positioning technique incorporating RF and ultrasound signals is proposed with the advantages of low complexity and compact size. A tag is attached to an interested object and the tag can communicate using ultrasound and RF signals. From the time of arrival (TOA) of the ultrasound, range information can be acquired at the interrogator. From the previously introduced RF DF techniques, the direction of the tag relative to the interrogator can be estimated. Therefore, the tagged inventory can be localized with real-time range and direction information.

II. Detailed Summary of Research Accomplishments

Several research projects regarding the biologically inspired RF direction finding program have been carried out including two-element planar inverted F antennas (PIFA) for RF direction finding, 3-D direction of arrival estimation with two antennas, high dielectric scatterer for electrical small antenna array with enhanced directional sensitivity, single antenna direction finding inspired by monaural sound localization, a leaky wave antenna based single element direction finding, 3-D luneburg lens based high accuracy direction finding, and portable radio frequency and ultrasound hybrid system for inventory localization. Detailed information of each of the projects is reported in the following sub-section.

A. Biological Inspired Two-Element Planar Inverted F Antennas (PIFA) for RF Direction Finding

Inspired by the human auditory system, an improved DoA technique using only two antennas with a scatterer in between them to achieve additional magnitude cues has been proposed. A Planar Inverted-F Antenna (PIFA) is chosen as a low profile receiving antenna widely used in wireless communication. The two-PIFA system is designed with a center frequency of 2.4 GHz and is fabricated and tested. The scatterer in between is optimized so that a 360º range of DoA estimation in the azimuth can be achieved. With the phase and magnitude difference information of the received signals at the two PIFAs, multiple signal classification (MUSIC) algorithm is applied to calculate the DoA under the assumption of additive Gaussian white noises. Figure 4 shows the measurement setup with the optimized PIFA / scatterer DF system. The measurement result of the angle estimation error is also plotted in Fig. 4. Large estimation error peaks appear at the incident angles where the received power level is low, indicating that further optimization is needed to achieve a robust DF system of high SNR without any ambiguity.

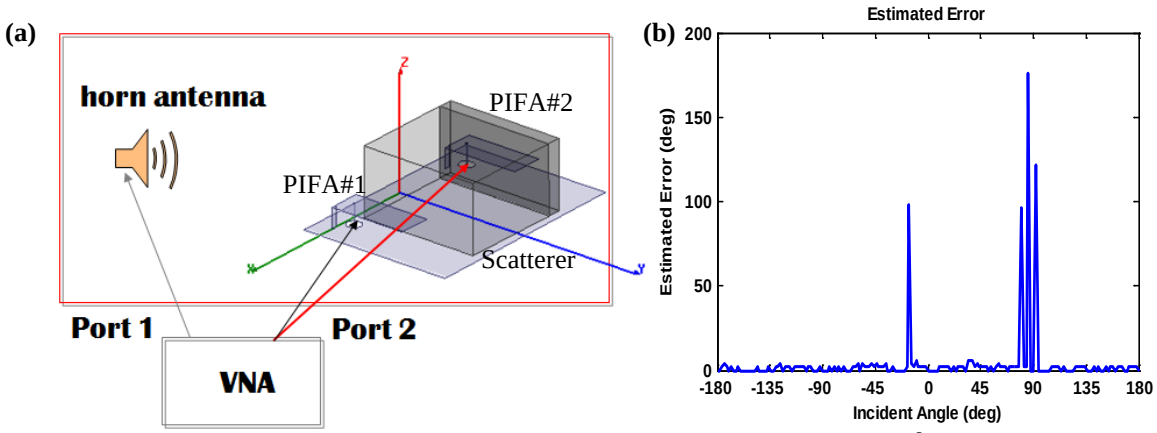

Figure 4. Two PIFA/scatterer (block #1: ARC-LS-10211, size 30.169 × 35.056 × 20 mm^3, ε_r = 2.05, μ_r = 1.19, tanδ = 1.15; block#2: ARC-LS-10211-25, size 4 × 35.056 × 20 mm^3, ε_r = 2.05, μ_r = 1.19, tanδ = 20) passive microwave direction finding configuration and measurement setup (a); Measurement results of the estimation error at 2.4 GHz using vector network analyzer (b).

B. 3-D Direction of Arrival Estimation with Two Antennas

The essence of the direction finding technique using two antennas with a scatterer in between inspired by human auditory system is to engineer the incident angle dependent phase and amplitude information for optimal sensitivity. From the previous 2-D direction finding analysis, it is obvious that the scatterer geometry and material parameters matter much in the DoA estimation accuracy. If the scatter is optimized such that the receiving response function is incident angle dependent for all directions including azimuth and elevation, this technique may be extended to achieve 3-D DF. As shown in Fig. 5, the original asymmetric scatterer (ε_r = 2.05 and tanδ = 1.15) from two monopoles / lossy scatterer system working at X band is divided into 5 × 4 × 3 = 60 blocks with every block of 3 mm^3. "1" represents the lossy block exists and "0" means a substitute of air in place of the lossy block. Thus every sequence of 60 binary digits represents one kind of scatterer geometry. Genetic algorithm is applied to optimize the scatterer geometry for the 3-D DoA estimation. Figure 5 also illustrates the procedure of this optimization. Figure 6 (a) illustrates a genetic algorithm optimized scatter for achieving 3-D DoA estimation. With this configuration, the estimated error of the polar angle - θ and the azimuthal angle - ϕ as a function of the incident angle (θ, ϕ) are shown in Fig. 6 (b, c). The simulated results of the 3-D DoA estimation have shown an encouraging accuracy and sensitivity by incorporating a 3-D optimized scatterer.

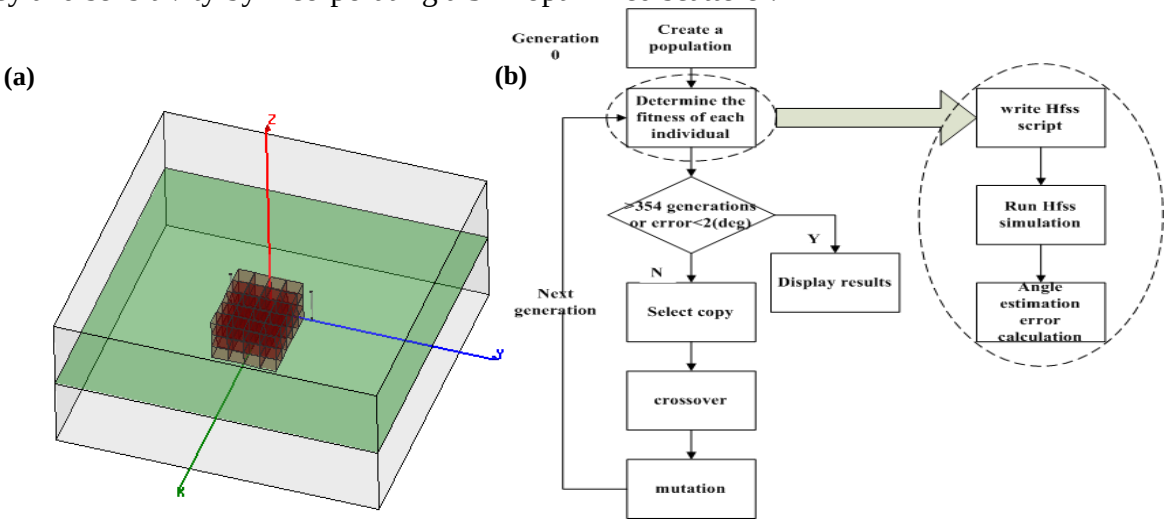

Figure 5. Original geometry of the monopole / scatterer system at X band (monopole length: 7 mm, spacing: 15 mm; scatterer size 15 × 12 × 9 mm^3, ε_r = 2.05, tanδ = 1.15) (a); Genetic optimization procedure (b).

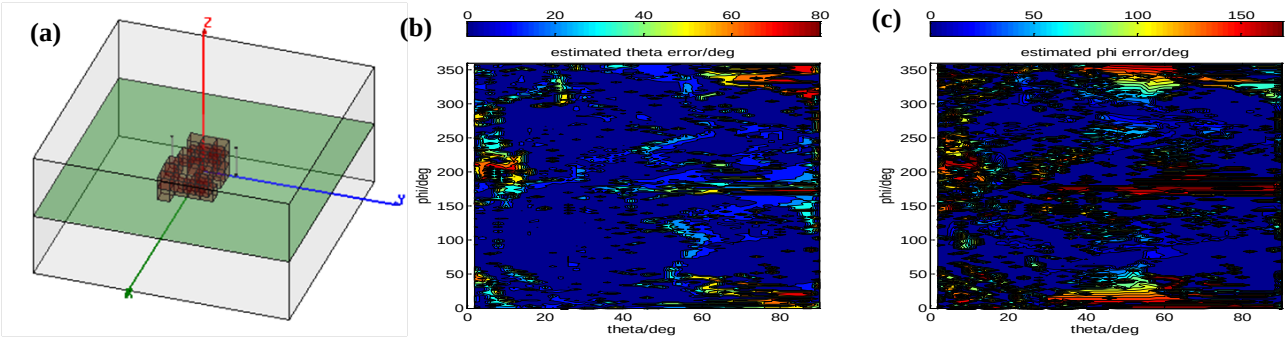

Figure 6. A GA optimized scatter for two-antenna 3-D DoA estimation (a), DoA estimation error of the polar angle - theta (b) and of the azimuthal angle – phi (c)

C. High Dielectric Scatterer for Electrical Small Antenna Array with Enhanced Directional Sensitivity

Electrically small antenna array with small spacing between any two adjacent antennas is attractive because of the compact size of the whole system. With the incident angle dependent phase difference information of the received signal at the antennas, DOA can be estimated accordingly. However, the phase difference can be very small due to the space limitation. The challenge is how to achieve high accuracy of DOA estimation under this circumstance. Inspired by human auditory system, a DoA sensitivity enhancement technique using two electrical small antennas and a high dielectric constant head-like scatterer in between is proposed to have amplified phase difference. The system demonstrates enhanced directional sensitivity for incident DoA estimation compared with conventional array with the same aperture size. Two closely-spaced electrically small monopoles' system (monopole spacing<< half wavelength, monopole length << quarter wavelength) is utilized where the corresponding phase difference between the received signals at the two antennas is very small ($\sim 2\pi d\sin(\theta)/\lambda_0$ with d – spacing, θ - incident angle relative to boresight and λ_0 - free space wavelength). After adding a high-dielectric-constant block in between the two antennas, the direction finding sensitivity can be increased. The system schematic is shown in Fig. 7. As one can see in Fig. 7, the received phase difference between the two monopoles is much greater for the case with the high dielectric constant (ε_r = 80.2, $\tan\delta$ = 0.01663) scatterer compared to that for the case without the scatterer, indicating an increased sensitivity for direction finding. However, there is a tradeoff for the DF sensitivity and the detection range. As shown in Fig. 7, after adding the scatterer, the received power of both antennas is lower. A design with better port impedance matching is shown in Fig. 8 with monopoles embedded in scatter 2. In this case, the phase difference is greater and the received power is much higher than that of the design without scatterer and with scatterer 1 in Fig. 7. Figure 9 shows another structure of scatterer used in the two -monopole direction finding system that is important. The simulated power level of this new design is still higher than that of the design without scatterer. The phase difference cue is nearly zero while the magnitude difference information can be used as the directional cue for this case instead.

Because both the electrically-small antennas size and electrically-small antenna spacing (mutual coupling between antennas cannot be ignored) contribute to the complex antenna input impedance, matching network for the system is needed to gain good system SNR. However, matching networks may alter the coupling between the two antennas, thus the system directional sensitivity may also be affected. Thus, it is essential to study the impact of the matching networks on the direction finding sensitivity to obtain a system that can achieve good directional sensitivity and good SNR at the same time so that high DoA estimation accuracy can be achieved. Matching approaches such as self-conjugate match (SCM), Eigen-mode decoupling match (EDM) and multi-port conjugate match (MCM) are widely used to enhance system SNR, especially for electrically small antennas . Self-conjugate matching method matches each monopole separately with the reflection coefficient of the matching circuits ($S_{3'3'}$, $S_{4'4'}$) and the monopoles (S_{11}, S_{22}) having the relationship of $S_{3'3'} = S_{11}^*$ and $S_{4'4'} = S_{22}^*$. Eigen-mode decoupling matching network consists of a 180-degree hybrid coupler right after the system to decouple the output two ports and two self-conjugate

matching circuits following the hybrid coupler. Multi-port conjugate matching network is to conjugate match the two monopoles as a whole, where the output reflection coefficient matrix of the 4-port matching network ($[S_{RR}]$) and the input reflection coefficient matrix of the monopole system ($[S_{ant}]$) has the relationship of $[S_{RR}] = [S_{ant}]^+$ ($[]^+$ denotes conjugate transpose). Direction finding performance of the proposed system using these matching networks is studied and evaluated. The models and simulation results are shown in Figs. 10 - 12. It is found that the simple self-conjugate match can increase the received power level by around 8 dB while maintaining the phase sensitivity. With the Eigen-mode decoupling match, the DF system has no phase information any more but the magnitude difference cue is enlarged. Multiport conjugate match can achieve the same high phase sensitivity and highest received power, which is around 32 dB more than the case without matching. In addition, the performance of the system with or without scatterer using general matching circuit that is lossless, reciprocal, and symmetrical is studied and compared. For a given lower bound of the received power at the two monopoles from all incident angles, optimal phase cue sensitivity is obtained by optimizing the s parameters of the matching network using MATLAB optimization. Here the phase cue sensitivity is the slope of the curve of phase difference vs. incident angle. The simulation results of the optimal phase cue sensitivity vs. power constraint indicate that there is a tradeoff between the received power and the phase cue sensitivity. Moreover, with scatterer system has higher phase cue sensitivity (increase of 0.3) compared with the case without scatterer under the same received power constraint. Both with and without scatterer cases have a maximum available power limit as marked in Fig. 13(b), which exactly corresponds to the results using multi-port conjugate matching network.

For experimental verification, the monopoles with a commercially available K50 high-dielectric block from TCI Ceramics in between are fabricated. The SCM network made of inductor-capacitor (LC) circuit is synthesized from the s parameters of the monopoles DF system at 300 MHz initially. Then the circuit is fabricated using RT/duroid 5880 laminate of 31-mil thickness. The final fabricated circuit board works at shifted lower frequency due to the existence of the microstrip line connecting the LC circuits to the two monopoles / scatterer system. Experiment is performed with VERT400 monopoles as the transmitter, and the two monopoles / scatterer with or without SCM circuit as the device under test. Vector network analyzer is used as the test equipment. The distance between the transmitter and receiver is about 3 meters to guarantee far field condition. Figure 14(b) is the measurement setup of the two monopoles / scatterer with SCM circuit mounted on the rotator. The measured received power and phase cue sensitivity vs. frequency for both with and without matching are plotted in Fig. 15(c)(d). As shown in Fig. 14, the self-conjugate matching is realized at 218.5 MHz where the system with SCM circuit has 10 dB larger received power from the two monopoles (averaged over incident angle) and same phase cue sensitivity compared with that of the case without matching as expected. However, as indicated from Fig. 14(d), the phase cue sensitivity of the system with SCM circuit has a sharp change at the self-conjugate frequency. The practical working frequency using this matching circuit should be at the lower frequency band of 215 MHz to 218 MHz to achieve better performance. In general, the incorporation of a high dielectric constant scatterer in between two electrically small antennas can lead to a directional sensitivity enhancement. In addition, the system can achieve both good SNR and enhanced directional sensitivity using some matching networks. This system is attractive for realizing portable DF system.

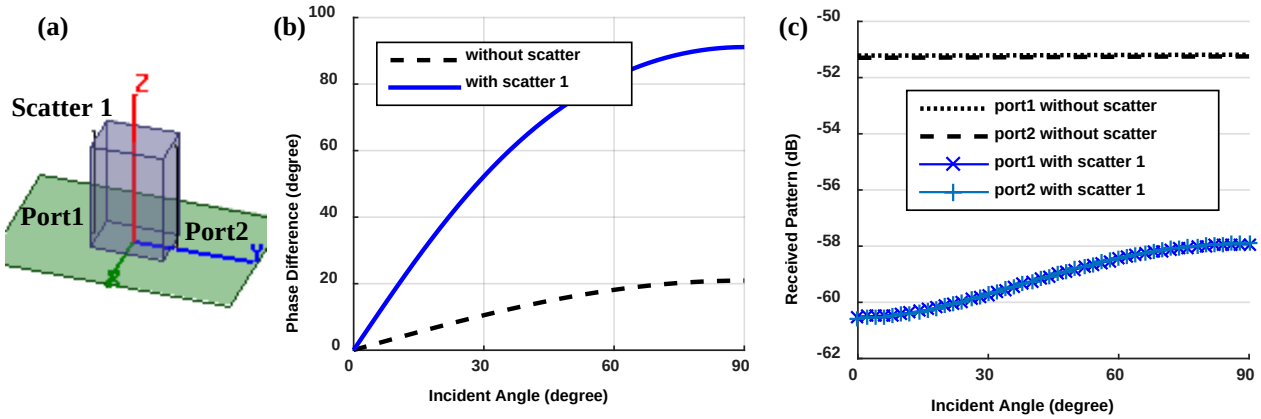

Figure 7. The schematic of 2 monopoles (monopoles length: 70mm, spacing: 50mm, ground size: 100 × 150 mm^2) with center scatterer of deionized water (ε_r = 80.2, tanδ = 0.01663, at 300 MHz) of a size of 30 × 44 × 70 mm^3 in between (a); the phase difference (b) and the received pattern (c) at 300 MHz for the DF system with / without scatterer 1.

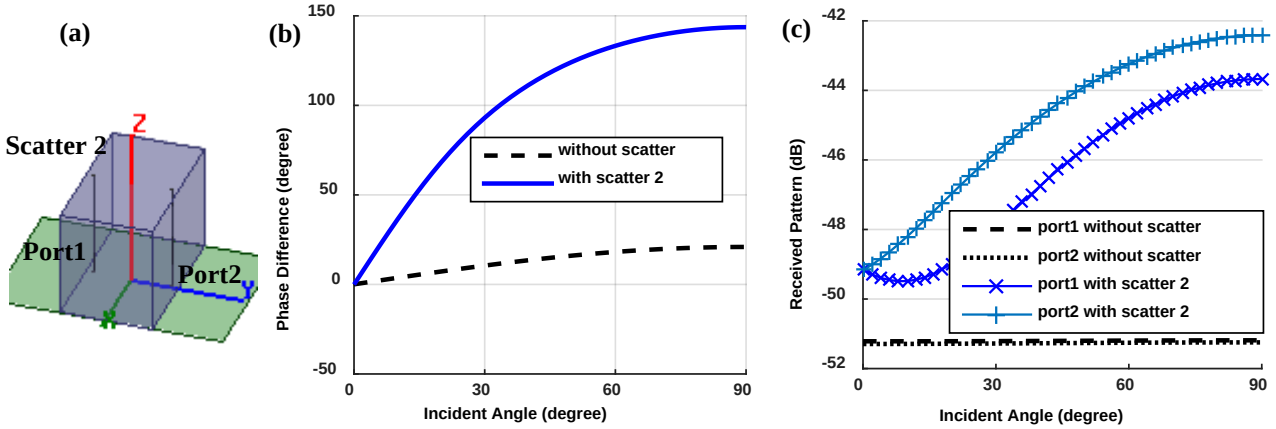

Figure 8. The schematic of 2 monopoles (monopoles length: 70 mm, spacing: 50 mm, ground size: 100 × 150 mm^2) with center scatterer of deionized water of a size of 100 × 60 × 70 mm^3 in between (a); the phase difference (b) and the received pattern (c) at 300 MHz for the DF system with / without scatterer 2.

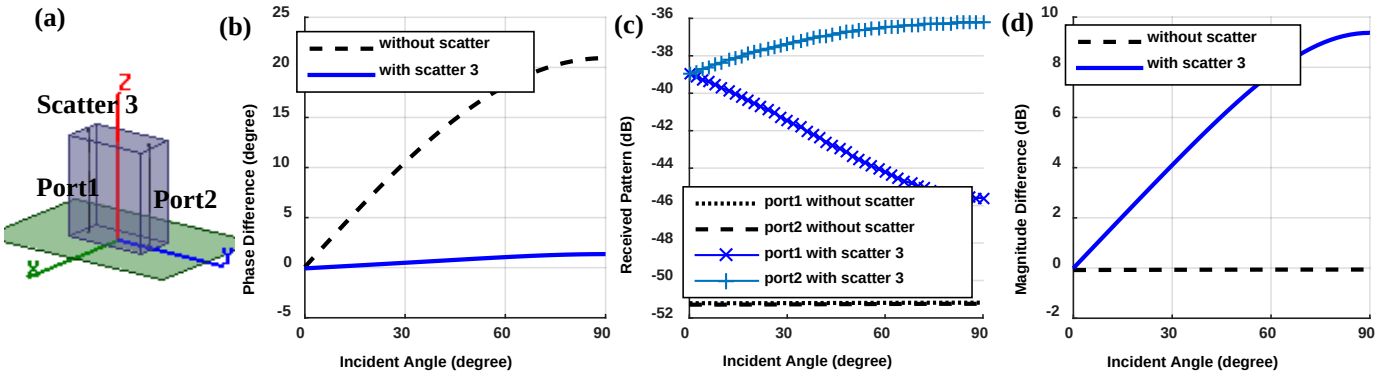

Figure 9. The schematic of 2 monopoles (monopoles length: 70 mm, spacing: 50 mm, ground size: 100 × 150 mm^2) with center scatterer of deionized water of a size of 30 × 60 × 70 mm^3 (a); the phase difference (b), the received pattern (c), and the magnitude difference (d) at 300 MHz for the DF system with / without scatterer 3;

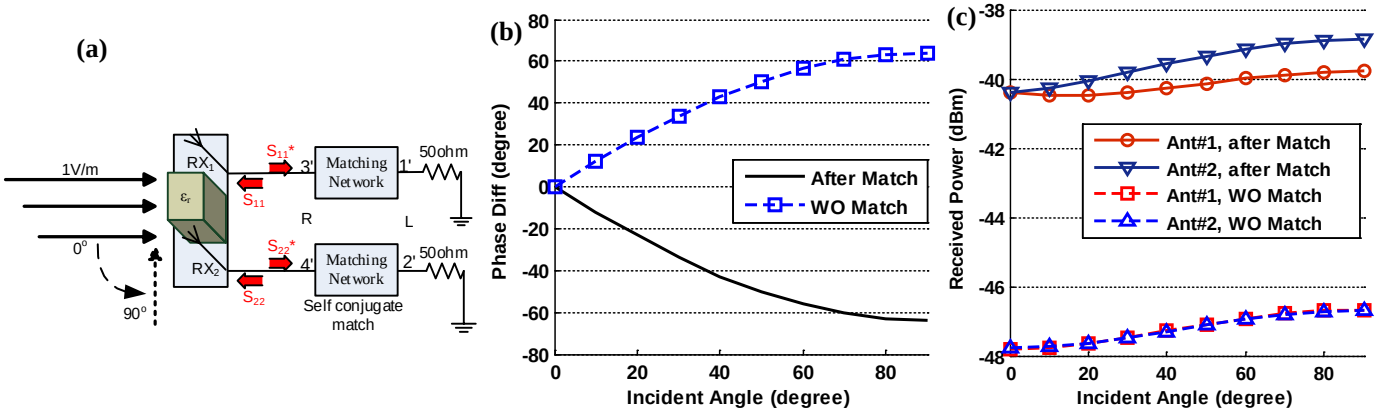

Figure 10. Schematic of monopole (monopoles length: 70 mm, spacing: 50 mm, ground size: 150 × 200 mm^2) with center scatterer (30 × 44 × 70 mm^3, TiO_2 anatase grade with ε_r = 48 & tanδ = 0.002) and self-conjugate matching network (a); The phase difference between two monopoles (b) and the received power at two monopoles (c) at 300MHz with / without matching.

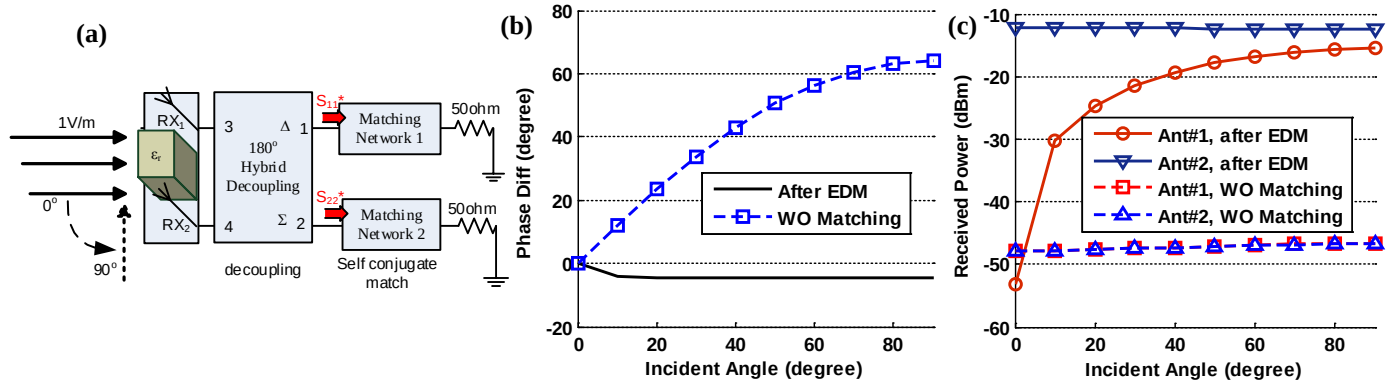

Figure 11. Schematic of monopole with TiO_2 scatterer and Eigen-mode decoupling matching (EDM) network (a); The phase difference between two monopoles (b) and received power at two monopoles (c) at 300MHz with / without matching.

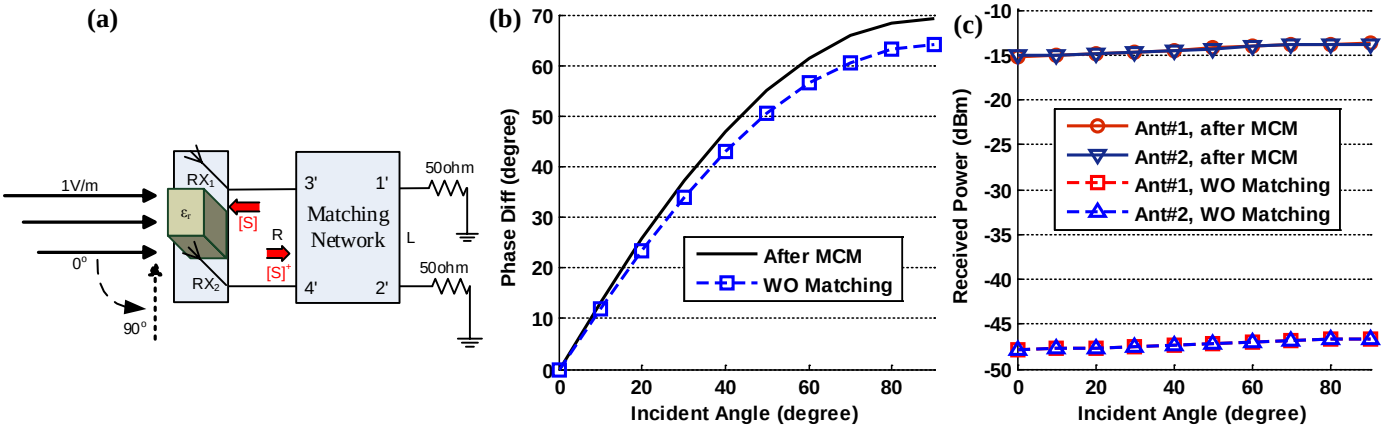

Figure 12. Schematic of monopole with TiO_2 scatterer and multi-port conjugate matching (MCM) network (a); The phase difference between two monopoles (b) and received power at two monopoles (c) at 300MHz with / without matching.

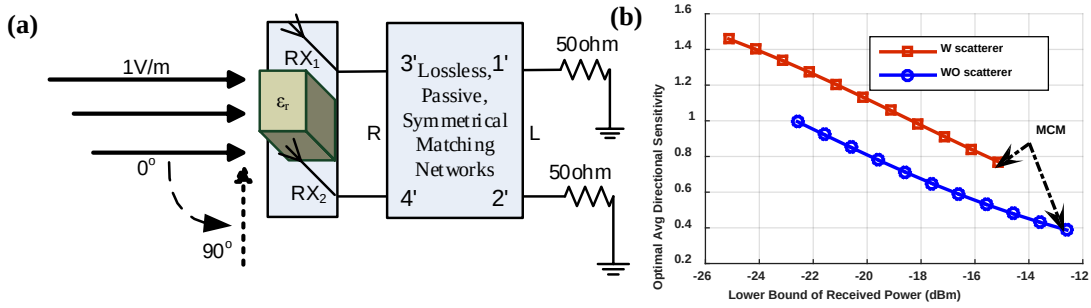

Figure 13. Schematic of monopole with TiO_2 scatterer and general lossless passive symmetrical matching networks (a); Power directional sensitivity tradeoff relationship after optimal matching network at 300 MHz (b).

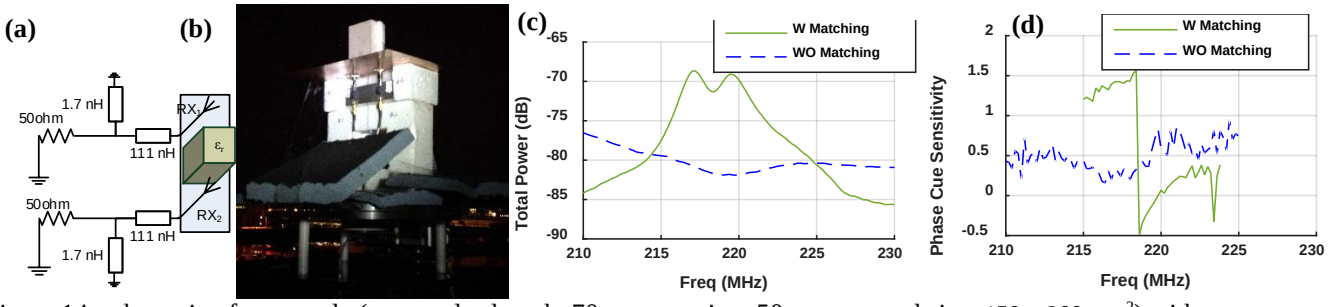

Figure 14. schematic of monopole (monopoles length: 70 mm, spacing: 50 mm, ground size: 150 × 200 mm^2) with center scatterer (30 × 44 × 70 mm^3, K50 with ε_r = 50 and tanδ = 0.001) and self-conjugate matching circuit (a) ; measurement setup (b); the measured total received power (c) and phase cue sensitivity (d).

D. Single Antenna Direction Finding Inspired by Monaural Sound Localization

A novel DoA technique for broadband microwave signals is proposed using a single Ultra-Wide-Band (UWB) antenna, inspired by the sound source localization ability of human auditory system using just one ear (monaural localization). The DoA of a broadband microwave signal is estimated by calculating the correlation coefficient between the received spectra of a wide-band antenna and the pre-saved incident angle dependent frequency response. The DoA estimation accuracies are evaluated for various antenna configurations and microwave signals with different signal-to-noise ratios (SNR). Verification experiments are successfully carried out and correspond reasonably well with simulation results. Figure 15 shows two designed UWB antennas working from 3 – 10 GHz for the proposed single antenna direction finding. The comparison of the simulated root mean square (RMS) error results of the two antennas are shown in Fig. 16 at different maximum SNR (SNR when the received signal is coming from the maximum radiation direction of the antenna - z direction) levels. Figure 16(a) plots the Root Mean Square (RMS) of the estimation errors of incident angles in the *x-y* plane for H-field in the *z* direction for different SNRs, which are calculated by running the simulation 1000 times. The estimation errors are less than 6º with most incident angles for SNR ≥ 15 dB cases. With the decrease of SNR, the RMS of the estimation error increases due to the influence of the noise. This is quite similar to the human monaural sound localization performance. The high estimation errors around 0º and 180º when SNR ≤ 15 dB are due to relatively low received power levels at these angles (~20dB lower than the maximum possible received power of the antenna). Similarly, the received spectra of the UWB antenna in the *x-z* plane for H-field in the *y* direction, and in the *y-z* plane with E-field in the *x* direction are also direction dependent, to different degrees. For co-polarization in the x-z plane (Fig. 16(b)), the estimation errors are less than 10º for most angles with SNR ≥ 20 dB. When SNR < 20dB, large estimation errors occur. Large peaks of error around +/- 90º are due to the fact that the received power level is low at those angles (same as spectra around 0º and 180º for x-y plane). Large error peaks around 0º and 180º are due to the relatively small angular dependence of the spectra (structure symmetry). For the incident wave in the *y-z* plane with E-field in the x direction (Fig. 16(c)), the received power level is large for all the angles compared with other polarizations. The RMS estimation errors are smaller than 30º when SNR ≥ 15dB. There is almost no region for low estimation errors when SNR is low (SNR = 10dB) because of the relatively small angular dependence of the spectra. Due to its symmetry with respect to the *x*-axis, the spectra of the elliptical UWB antenna with added noise are also correlated to the original spectra along the symmetric direction with respect to the *x*-axis plane (i.e., θ and -θ). To break this symmetry to increase the estimation accuracy, another UWB antenna with a D-shaped configuration is also designed, as shown in Fig. 15(b). Following the same DoA estimation procedure described previously, the RMS of the estimation errors with different SNRs are plotted in Fig. 16(d) for the case of incident wave in the *x-y* plane with the H-field in the *z* direction. The correlation coefficients at the symmetric direction with respect to the *x*-axis are reduced due to the break of symmetry of the D-shaped antenna, leading to improved estimation accuracy. The RMS of the estimation error is less than 6° for SNR ≥ 15dB and better than the case of elliptical antenna (when SNR = 15 dB, averaged RMS error for D-

shaped antenna case is 2° while elliptical antenna case is 5°). The higher RMS errors around 0° and 180° are due to lower received power level. Figure 16 (e) and (f) plot the RMS errors when the incident waves are in the x-z plane (H-field in the *y* direction) and *y-z* plane (E-field in the *x* direction) respectively. For the case of the incident wave in the *x-z* plane with co-polarization, the RMS errors have peaks around 0°, 180° and +/-90° because of the same reason as the elliptical antenna case. Due to the break of symmetry respect to x axis, the RMS errors for the *y-z* plane is lower compared with elliptical antenna case for most incident angles, except for around 0° and 180° where symmetry respect to y axis still exists.

To verify the DoA estimation technique using a single UWB antenna experimentally, the two UWB antennas discussed are fabricated and tested. Figure 17 shows the experimental setup. The UWB receiver is placed 5.3 m away from the transmitter (in the far field range of the transmitter) as shown in Fig. 17(a). Continuous wave (CW) frequency sweeping is applied for the transmitted signal to obtain broadband spectra. However, in practice the system is applicable for broadband pulse signal with relatively flat frequency spectra. The source signal can have arbitrary frequency response if the transmitted waveform is known at the receiver a priori. The received spectra are measured for both UWB antennas in different planes for different polarizations with a 1 - 18 GHz ridged horn antenna as the transmitting antenna (the transmitting power is +10 dBm). The UWB antennas are placed on the positioning system and rotated from -180º to 180º with 2º step horizontally. Figure 17 (b-d) illustrate the views of the receiving antenna mounted for the measurement in the x-y plane, the x-z plane and the y-z plane. Two sets of spectra as a function of incident angles are measured at different locations as the calibration data and testing data respectively. The estimated incident angle in testing is calculated by finding the angle with peak correlation coefficients between the tested spectrum and the pre-saved calibration spectra. When the incident wave is from z direction and E field from the x direction, the received SNR is approximately 10 – 15 dB. The measured spectra are distorted somewhat comparing to simulation which might be due to the following factors, first, the scattering of the feeding cable of the receiving antenna; second, the frequency dependent fading due to the multipath effect of the environment; and last, the frequency response of the transmitting horn antenna. As shown in Fig. 17, the directly transmitted signals reaching the receiver are also incident onto the connected cables, potentially causing scattering and distorting the measured spectra. Because of the existence of the side walls and ground, there may be frequency dependent fading due to multipath effects. At last, the gain of the double-ridged horn antenna used in the experiment is frequency dependent throughout the tested band, thus has impact on the received spectra. Smoothing process, though cannot remove spectra distortion introduced above, can reduce uncorrelated noises like GWN. Smoothing is processed with 11 points width in the test. Figure 18 plots the measurement results of co-polarized incident signals at different planes for both antennas. For the elliptical antenna, the measured estimation errors are less than 6°. The DoA estimation errors of the D-shaped antenna are less than 4° for most cases. The large estimation errors at 0° and 180° for the x-y plane with H field in the z direction (Fig. 18(d)) and at +/-90° for the x-z plane with H field in the y direction (Fig. 18(e)) correspond with small received power at these angles (radiation nulls). The elliptical antenna also has this issue. Simulation results successfully predict these peak estimation errors. Other than those angles, the D-shaped antenna has similar estimation performance compared to the elliptical antenna for x-y and x-z planes. Compared to the elliptical antenna, the D-shaped UWB antenna has better angle estimation performance for the y-z plane with E-field in the x direction due to symmetry broken as shown in Fig. 18(f). In general, the feasibility of reasonable DoA estimation using a single UWB antenna is verified.

The feasibility of the single antenna DoA technique is demonstrated in both simulations and experiments. Compared to previous work using two antennas and MUSIC algorithm which achieved 1º to 2º accuracy, this single antenna approach has the advantages of requiring less hardware components and less computational intensity (no eigen-value calculations needed) at the expense of sacrificing some accuracy. This kind of biological inspired RF technique may lead to future novel direction finding systems that are low-cost, compact and light weight. Although with its advantages, before practical applications could be

widely implemented, several potential issues of this technique need to be addressed. First, our initial design (the elliptical antenna) indicates that good SNR is critical to obtain high DoA estimation accuracy using this technique due to some intrinsic symmetries of the antenna. Nevertheless, with an improved antenna design (D-shaped to break some of the symmetries), the DoA estimation performance is better compared to the elliptical UWB antenna under the same SNR conditions. It is likely that further improvement of the antenna design with higher incident angle dependent spectra can be achieved for better performance. In addition, although the UWB band (3.1 to 10.6 GHz) is used to demonstrate the idea here, the technique itself should work at other frequency bands as well so that higher SNR scenarios may be realized. One caveat of this technique is that it does require the user to know the sent signal a priori. Similarly, for the human auditory system, monaural DoA also only works when a white noise (or a close to white noise) is incident and / or after some self training. Therefore, for the microwave case, the transmitting antenna frequency response would contribute to the received spectrum. Thus it is critical to use a broadband source that is either more or less frequency independent emulating a white noise or has well known frequency response that can be taken into account at the receiving end. Third, as for any DoA technique, multipath effects will impact the DoA accuracy and are not specifically included in this work for initial feasibility study. For applications in an open space – grassland, schoolyard, military base land, etc., the multipath effect is weak and less important. In addition, a pulse based UWB system may be used which is less prone to multipath fading compared to a CW based system. And we have demonstrated such a pulse based system using a leaky wave antenna with high accuracy as shown in the following section. Nevertheless, more realistic multipath effects for specific system scenarios may need to be studied in more details for practical applications. Finally, in our experiments, the cable scattering may impact the resulting spectra, while in practical applications the placing of the feeding line should be carefully taken into consideration to eliminate this issue.

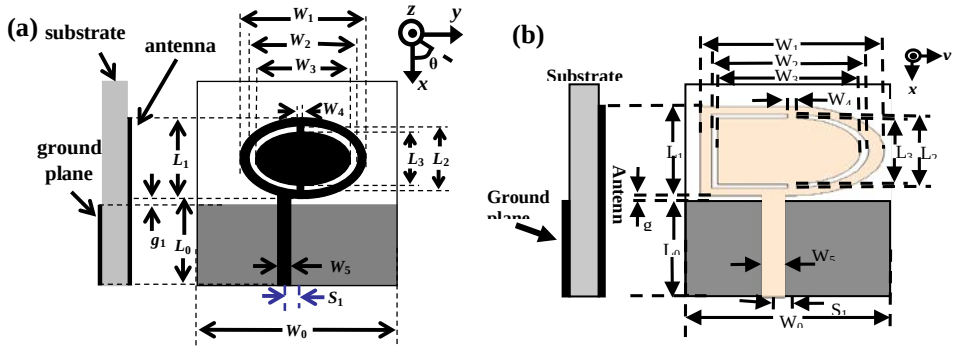

Figure 15. The UWB antennas for single antenna DF (elliptical antenna (a) and D-shaped antenna (b).

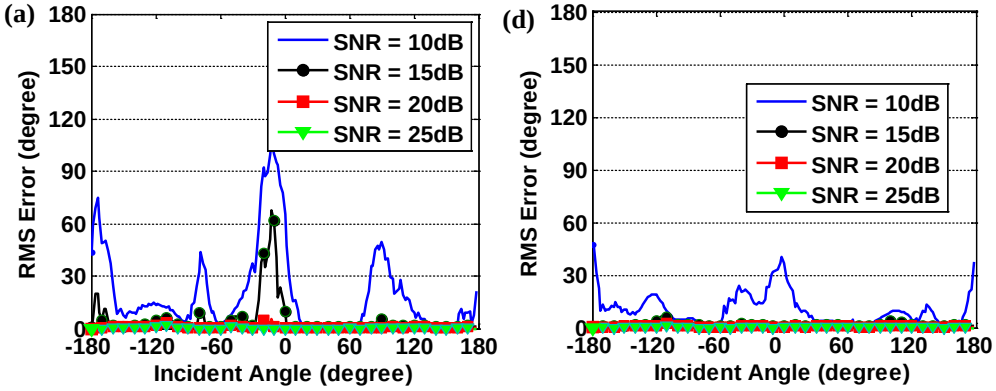

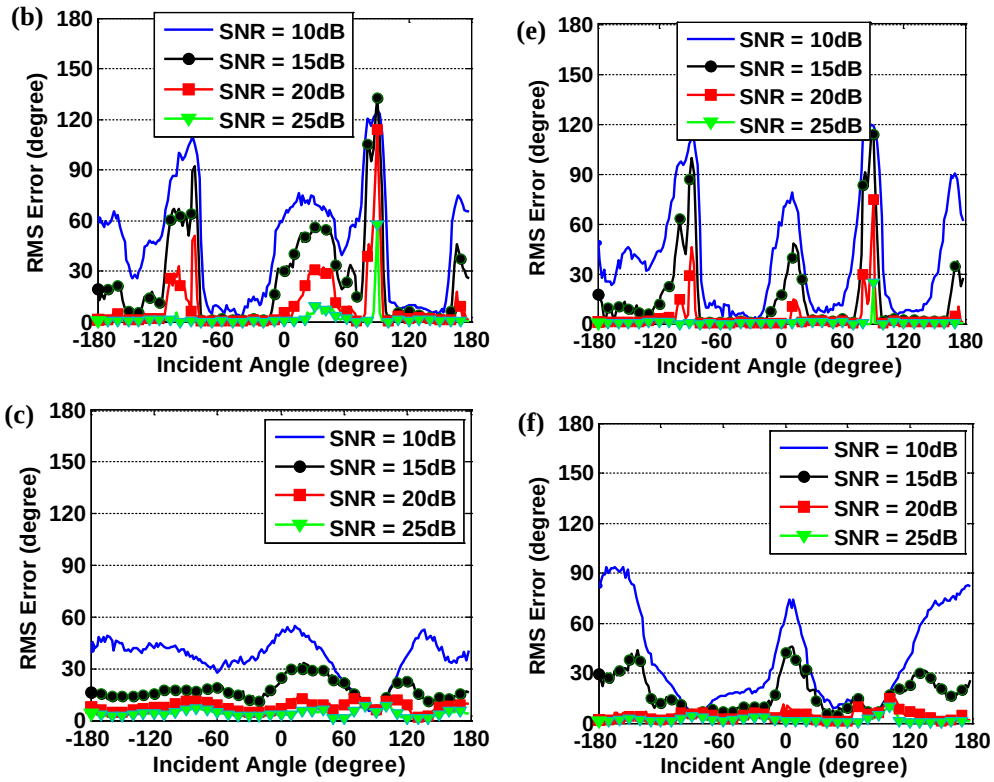

Figure 16. DoA performance of the RMS estimation errors for different antenna maximum SNR for the elliptical antenna (left) and the D-shaped antenna (right) respectively with the incident wave in (a, d) the *x*-*y* plane (with H-field in the *z* direction), (b, e) the *x*-*z* plane (with H-field in the *y* direction), and (c, f) the *y*-*z* plane (with E-field in the *x* direction).

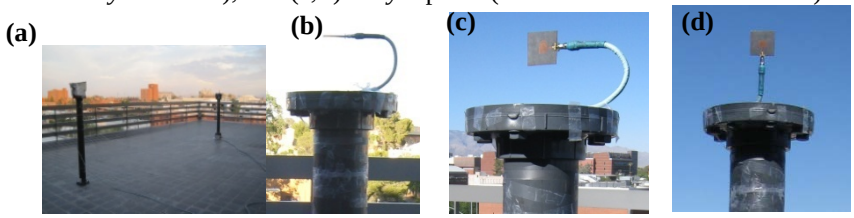

Figure 17. (a) UWB DF experiment setup; Receiver set up for angular sweeping in the x-y plane (b), the x-z plane (c), and the y-z plane (d).

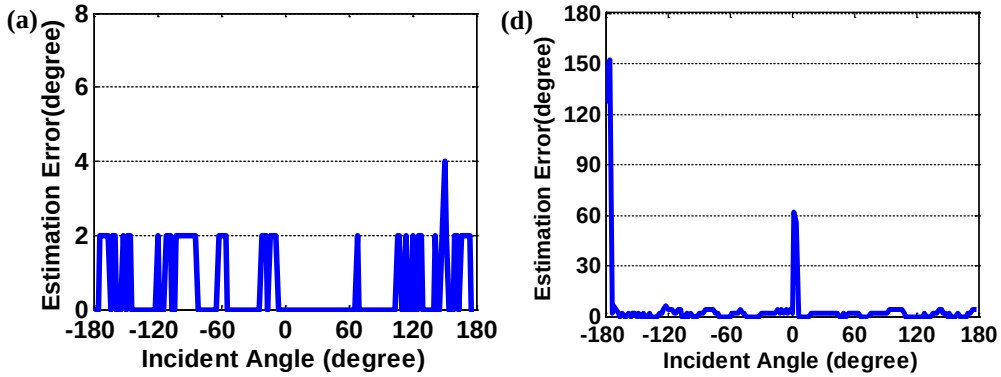

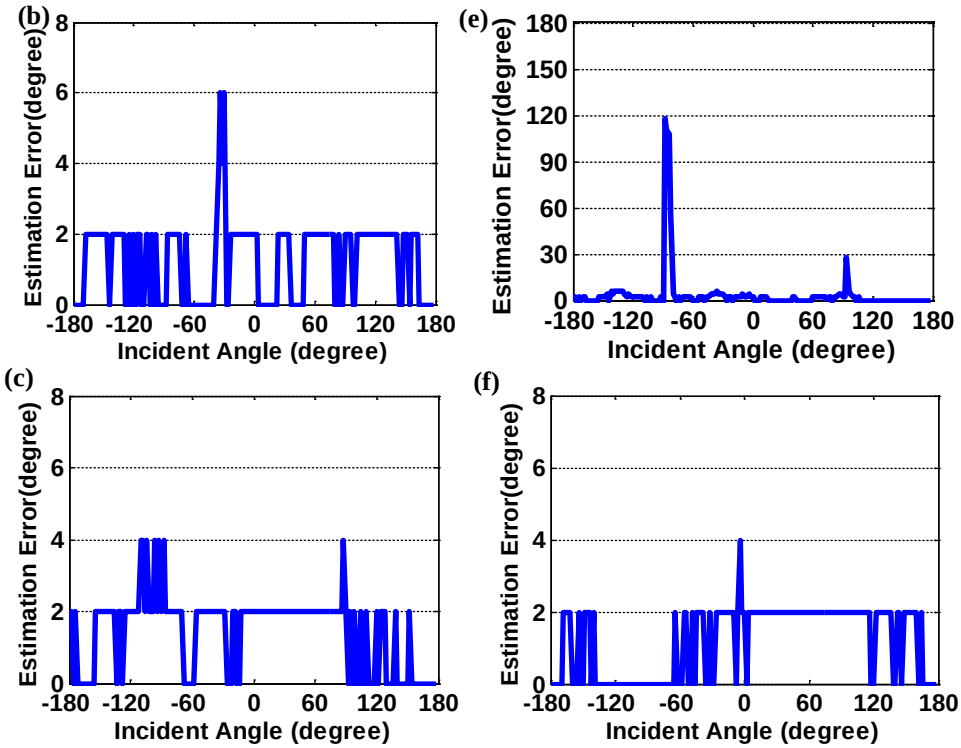

Figure 18. The measured estimation errors of the elliptical UWB antenna (left) and D-shaped antenna (right) respectively with the incident wave in (a, d) the *x*-*y* plane (with H-field in the *z* direction), (b, e) the *x*-*z* plane (with H-field in the *y* direction), and (c, f) the *y*-*z* plane (with E-field in the *x* direction).

E. A Leaky Wave Antenna Based Single Element Direction Finding

The single antenna DoA technique inspired by monaural (one ear) localization ability of human auditory system can have higher degree of estimation accuracy with improved SNR. A microstrip leaky wave antenna is designed which has good spectra cue sensitivity and high SNR within 90˚ incident angle range. The leaky wave antenna is fabricated and the broadband positioning system is designed as shown in Fig. 19. A Gaussian pulse with a bandwidth of 2 - 3.5 GHz is generated by an arbitrary waveform generator. The pulse is amplified and then transmitted by a standard horn antenna. The leaky wave antenna as the receiving antenna is designed in HFSS software and then fabricated with good matching and reasonable radiation efficiency in the interested band. The received signal is recorded by an oscilloscope and Fourier transform is performed for further data processing. Because of the main beam steering property of the leaky wave antenna over the working frequency range, by exploiting the incident angle dependent frequency response of the antenna, the DoA of a broadband microwave signal can be estimated with high accuracy. Figure 20 plots the measured spectra and the DoA estimation error. It can be observed that the error is less than 6º from 0º to 90º range, showing a good DoA performance. The relatively higher error at incident angle of 90º is due to the relatively small angular dependence and relatively low SNR.. The measured results have confirmed the feasibility of the proposed wideband DOA estimation technique. the proposed technique utilizing a microstrip leaky wave antenna is demonstrated with good DoA performance in 90˚ range .

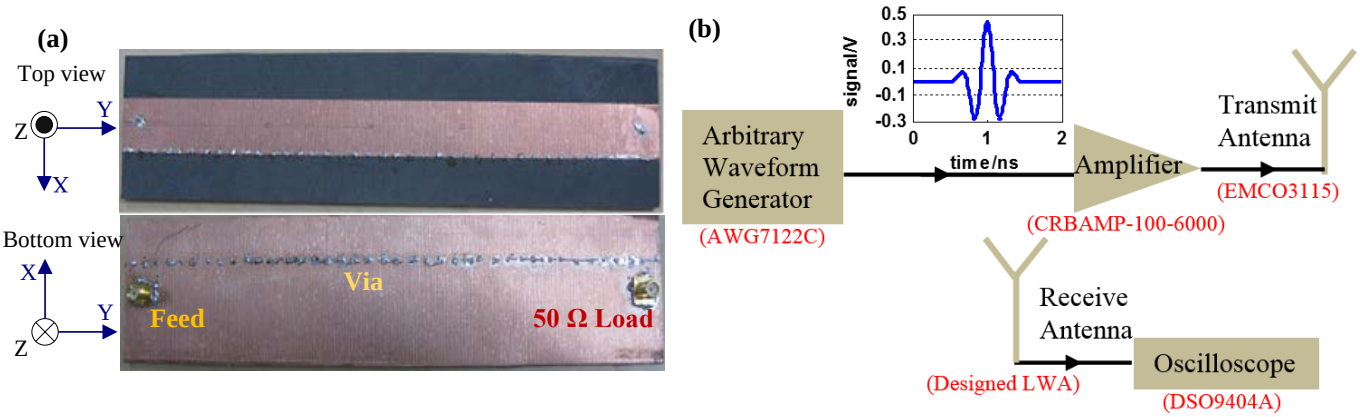

Figure 19. The top and bottom views of the fabricated leaky wave antenna (a); Schematic of the single leaky-wave antenna DF measurement setup (b).

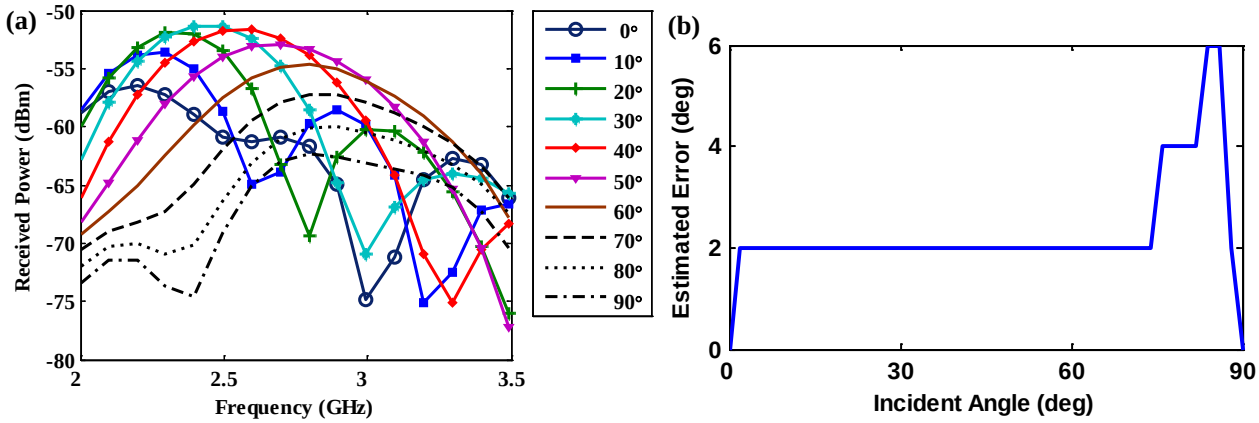

Figure 20. Measured spectra for θ from 0˚ to 90˚ in y-z plane with the E field in the x direction (a); measured DoA estimation error (b).

F. 3-D Luneburg Lens Based High Accuracy Direction Finding

Luneburg lens is a gradient index component that has the characteristic that every point on the surface of the lens is the focal point of a plane wave incident from the opposite side. It has the advantages of ultra wide bandwidth, high gain and multi-beam forming ability. A broadband passive direction finding system utilizing Luneburg lens has been investigated. When a number of detectors are mounted around a circle on the surface of a Luneburg lens as shown in Fig. 21(a), the received power distribution at the detectors is incident angle dependent. By utilizing the information of the received power distribution, the DoA can be determined. This novel direction finding system is advantageous in that it is wide banded and it does not require expensive phase shifter components. In addition, the high gain property of a Luneburg lens leads to small correlation between received power distributions for different incident angles, thus high accuracy for the incident angle estimation can be achieved. A correlation algorithm is used to achieve the DoA estimation. For incident plane wave from the azimuthal plane, the received power distribution at the detectors with Gaussian white noise was correlated to the pre-saved calibration set of data for all angles of incidence. The angle which has the largest correlation is the estimated direction of the incident wave. To quantitatively evaluate the performance of the proposed Luneburg lens direction finding system, the Cramér–Rao bound (CRB - a lower bound on the estimation error variance) of the DoA estimation error is also calculated. Figure 21(b) demonstrates the root mean square (RMS) errors of CRB and correlation method vs. SNR (averaged over all azimuthal angles) with 36 detectors uniformly placed on the surface of the lens at 10GHz. The RMS errors increase with decreasing SNR. For SNR > 15dB, the calculated RMS error using the correlation method is almost the same as the CRB (less than 2°) while for SNR<15dB, it increases sharply with further reduced SNR. It is concluded that the correlation method performs well for

high SNR environment and fails at heavily noisy background.

To demonstrate the proposed direction finding system, the Luneburg lens with 36 detectors mounted on its surface to receive the signal from all 360 degrees is measured at 5.6 GHz as shown in Fig. 22. The Luneburg lens is fabricated using the polymer jetting technology with a radius of 11.8 cm. Although the Luneburg lens used is broadband (at least from 3 – 12 GHz), without losing generality, an operating frequency of 5.6 GHz is selected at which the detectors have its peak sensitivity. In the experiment, a signal generator (Agilent E8257C) connected to a double ridged horn antenna is used as the transmitting source. A picture of the experiment setup for the direction finding is shown in Fig. 22(b). Thirty six detectors with a separation of 10 degrees are mounted on the surface of the lens in the tests. The distances from the transmitting horn to the Luneburg lens are 3 m and 4 m, for the calibration and the performance test, respectively (both in the far-field). The detector is made of a zero biased diode (SMS7630-061) fed by a monopole antenna printed on an 8-mil Duroid-RO4003C substrate. The direction finding results using the previously discussed correlation algorithm (Fig. 22(c)) show that the estimated error is smaller than 1 degree from all incident angles. Using the Luneburg lens direction finding system with fully populated detectors (i.e., 36 detectors with 10º separation), accurate DOA in the entire azimuth plane is obtained. If detectors are populated in a 3-D fashion on the lens surface, accurate 3-D direction finding can also be obtained. This kind of Luneburg lens based direction finding system may be a good candidate to achieve a portable, low cost and accurate direction finding system that will be useful for many applications.

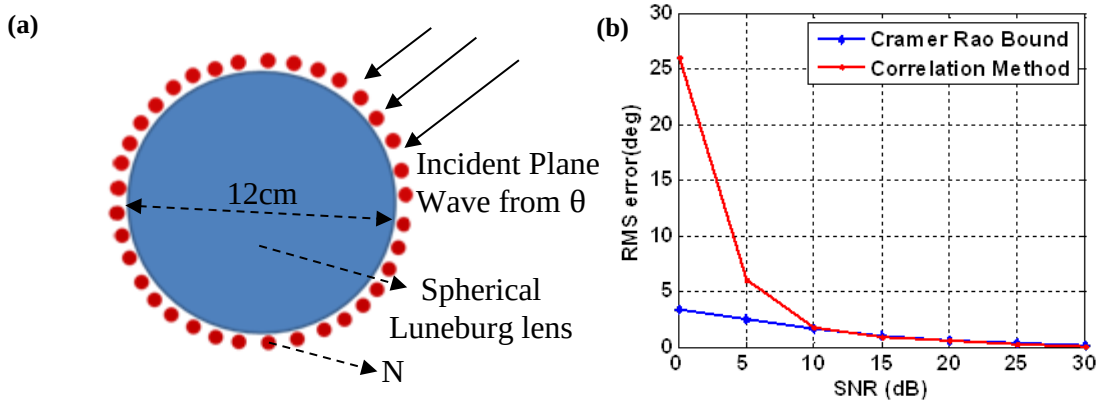

Figure 21. Schematic of a Luneburg lens based DF system (a) and simulated performance at 10 GHz when 36 detectors mounted on the surface of the Luneburg lens (b).

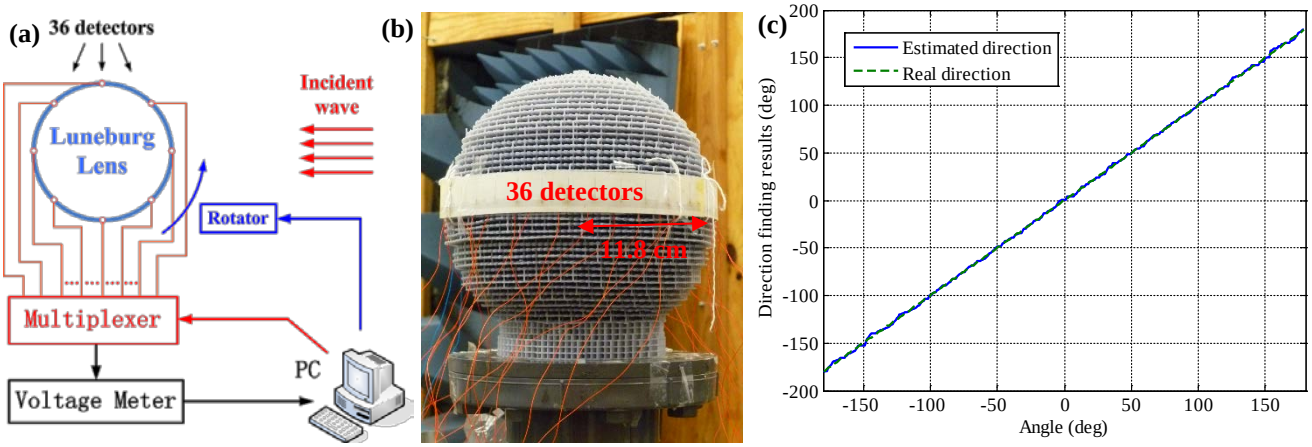

Figure 22. Schematic diagram of the experiment setup (a); Luneburg lens with 36 interrogators mounted around the surface (b); Estimated direction results at different incident angles from -180º to 180º(c).

G. Portable Radio Frequency and Ultrasound Hybrid System for Inventory Localization

In practice, localization in addition to direction finding is often in need. Inventory localization of items such as a book, a laptop, a package, or even a sheep is highly desirable. GPSs are popular in outdoor real-time localization scenario while the accuracy of them may not be sufficient for inventory localization applications. Here a novel low cost and portable localization system for inventory localization utilizing RF and ultrasound signals has been proposed and studied. By incorporating the distance (obtained from ultrasound) and the direction information (obtained from the RF antennas), the position of any target tag can be estimated. The description of the inventory localization system is shown in Fig. 23(a). A tag will be attached to any object or people whose location is to be detected. An interrogator will first send out a localization request signal and at the same time start a timer. After the tag receives the localization request, it will send out both RF and ultrasound signals. Once the ultrasound arrives at the interrogator, the timer will be stopped and recorded. The time difference of the recorded stop and start time at the timer will be used for distance estimation. The phase difference of the RF signal received at the two antennas of the interrogator will be used for DoA estimation. By incorporating the distance and DoA information, the location of the tag can be determined.

As a proof of concept, commercially available RF and ultrasonic devices have been chosen to demonstrate our prototyping technology. Within each device, the tag consists of a DIGI xbee pro s2, an ultrasonic transmitter (HC-SR04), and one microcontroller unit (MCU) - arduino duemilanove. The interrogator consists of one DIGI xbee s2, one ultrasonic receiver, one arduino, a pair of PIFAs (planar inverted-F antennas) DoA system, an oscilloscope (DSO9404A) and a personal computer (PC). As shown in Fig. 23(b), the interrogator will send out a localization request using 2450 MHz band, and the arduino at the interrogator mandates the xbee to emit an RF signal and to start the timer. Once the xbee at the tag receives the RF signal, the arduino at the tag will request the ultrasonic module to emit an ultrasound and the xbee to transmit an RF signal. At the interrogator, once the ultrasonic module detects the ultrasound, the timer will stop and the time difference will be calculated and sent to the PC. Once the PIFA DoA system detects the RF signal, the oscilloscope will start acquiring the waveforms. The phase difference of the received signals at the two PIFAs will be then calculated.

The performance of the localization in azimuth has been demonstrated through measurement. Figure 24 is a demonstration of the measurement setup. The noise level at the oscilloscope for this measurement is of -40 dBm, and the received SNR is 20~29 dB. The distance between the interrogator and the tag is around 87 inches (2.21 m). The estimated distance is post-calibrated by the measured distance when the true distance is zero. The direction of the tag relative to the interrogator is achieved using the phase difference of the received signals at the two-PIFAs. The phase difference vs. all incident angles in the azimuth is pre-saved for calibration using the average phase difference calculated from the measured data on various dates. At the tag-interrogator test, the phase difference of the received signals at the PIFAs at the interrogator is measured. The direction of the tag relative to the interrogator is obtained from checking the pre-saved library of phase difference vs. incident angle. . The estimated location vs. the real position of the tag relative to the interrogator is compared in Fig. 25 with 5 times of tests taken. The corresponding RMS error of all tests is also plotted in Fig. 25. The distance accuracy is limited within +/- 0.5m because of the noisy zigbee protocol used in the xbee. The xbee is always updating routes and checking for network connectivity before transmitting / receiving any data, which induces processing delays about milliseconds. However, if other simpler protocol like 802.15.4 is used, the distance estimation accuracy will be within several centimeters because the time deviation is usually within microseconds.

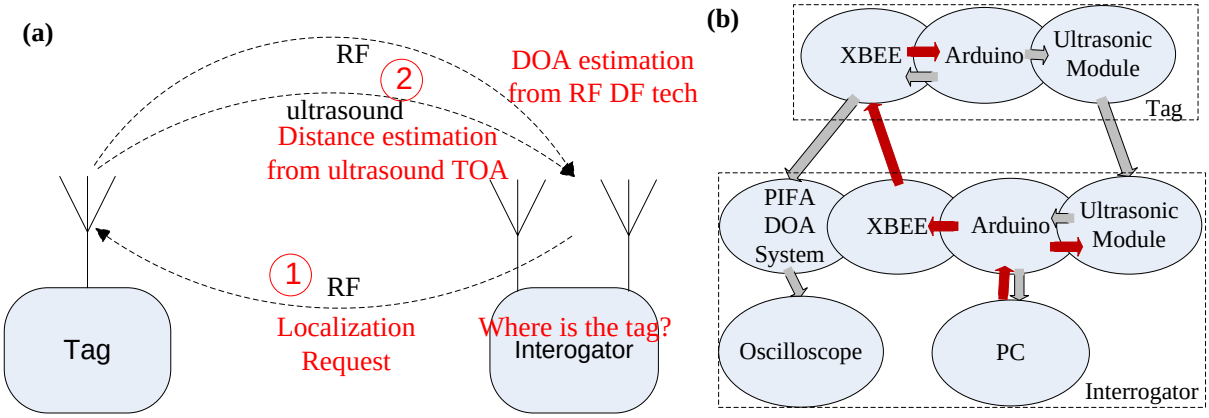

Figure 23. The schematic of the inventory localization system (a) and the lock diagram of the proof of concept system demonstration (b).

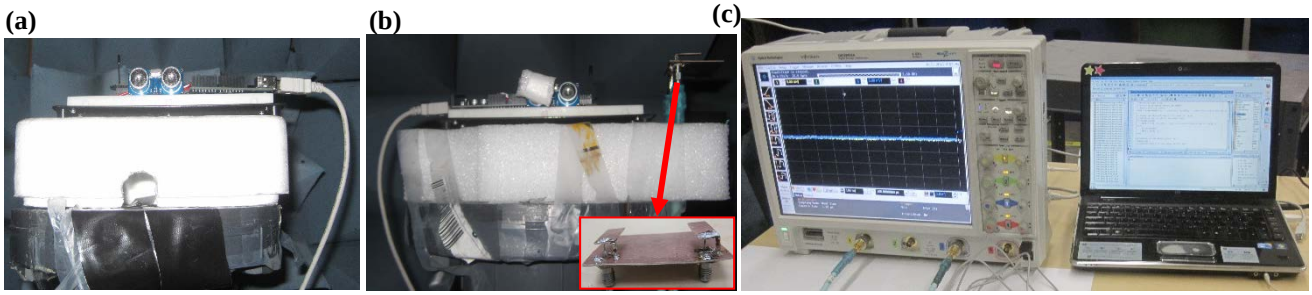

Figure 24. Measurement setup of the tag (a), the interrogator (b), and the signal processors (oscilloscope and laptop) for the interrogator (c)

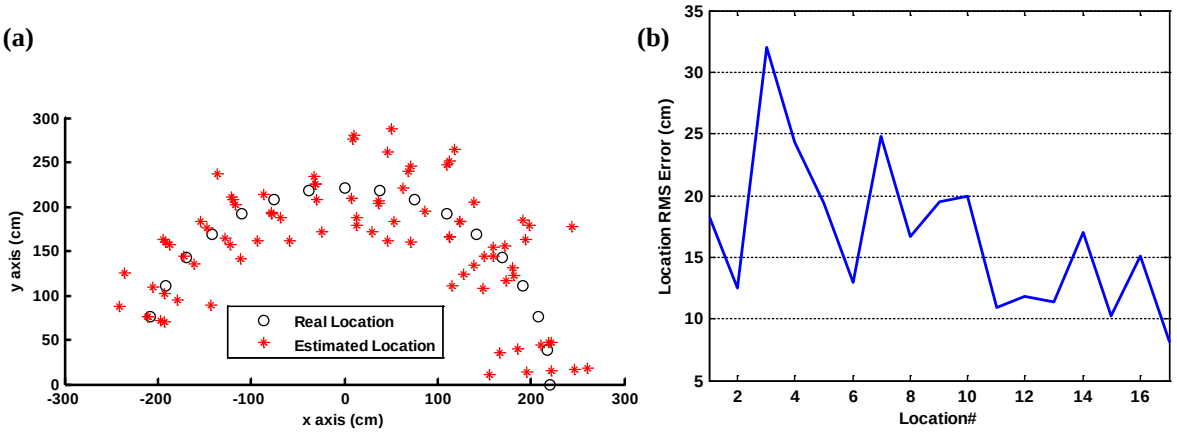

Figure 25. 2-D real position vs. estimated location (measured 5 times) (a) and location estimation root mean square (RMS) error (b).

III. Conclusions and Discussions

Human ears have the amazing ability of estimating arrival angle (mainly in the azimuth plane) with accuracy up to 1° without ambiguity under binaural (utilizing two ears) conditions. Inspired by the human auditory system, a low profile DoA system using two PIFA antennas with a scatter in between them, emulating the low-pass filtering function of the human head at high frequency to achieve additional magnitude cues, has been designed and tested. The results of azimuth DoA have shown that almost 360º range of DoA estimation in the azimuth plane can be achieved with high accuracy for continuous wave. This two antennas / scatterer DF system can be extended to 3-D DoA estimation. By applying genetic algorithm, the scatter in between two monopoles is optimized in terms of geometry and material parameters to satisfy that the response function is incident angle dependent for all directions in 3-D. Simulated 3-D DoA estimation errors of the optimized monopole/scatterer configuration show an encouraging accuracy

and sensitivity. However, the large DoA estimation error near ϕ=0° and 180° and θ=0° should be further studied and eliminated. One possible solution may be applying scatterer optimization of both geometry and more flexible material parameters including ε, μ, and tanδ. The fast developing 3D printing technologies with mixture of polymer and ceramic powder of high ε, μ or σ have enable the realization of flexible EM parameters and shape. Using other practical antennas with higher directivity instead of monopoles may also help. In addition, with the incorporation of a scatterer of very high permittivity, better DoA sensitivity is demonstrated compared to that of a conventional array with the same aperture size. The impact of the shape of the scatterer to the directional sensitivity is studied and a system of special scatterer structure with improved output SNR is proposed. Various matching circuits are studied to get good power level and good directional sensitivity at the same time. Self-conjugate match is simple but improvement of power level is little. Eigen-mode decoupling match is easy to design but only has magnitude difference cue instead of phase cue. One of the ports will have low SNR. Multi-port conjugate match is the best in that one can achieve maximum available power at the output with same phase cue sensitivity. But in general, there is a trade-off between the available power and the phase cue sensitivity. In addition, using optimized matching networks, two monopoles with high-permittivity scatterer configuration can achieve better phase cue sensitivity under the same power level constraint than that of whithout scatterer case . Inspired by human monaural direction finding capability, a technique using a single Ultra-Wide-Band (UWB) antenna for broadband microwave signals DoA estimation has been studied. The DoA estimation accuracies for various antenna configurations are evaluated with Gaussian White Noise for microwave signals comparable to the laboratory environment. Experiments are successfully tested with different antenna orientations. The measurement results correspond reasonably well with the simulation results. A pulse based 90°-range DoA estimation technique utilizing a microstrip leaky wave antenna has also been demonstrated. This DF system has good spectra sensitivity and high SNR for all incident angles in the range. In addition, a broadband passive direction finding system employing a broadband 3-D Luneburg lens with 36 detectors placed on the lens equator has been investigated. The experimental results show that the DoA estimation error is less than 1º for all 360º angles. At last, a portable localization system utilizing RF and ultrasound signals has been studied. As a proof of concept, commercially available RF and ultrasonic devices have been chosen to demonstrate the prototyping technology through measurement. Because of the limited capability of the proposed RF system, only 2-D position is estimated. However, the technique can no doubt be extended to a 3-D localization application if its 3-D directional estimation capability is enabled with a specially designed scatterer in between the two antennas.

Human auditory system has many other amazing capabilities. Cocktail party effect is one example. The phenomenon that people can be attentive to a specific person in a noisy party environment can be applied in solving multiple-signal DF or DF in a multipath rich environment. A possible configuration is to use two broadband antennas that incorporate both single-antenna and two antenna / scatterer DF techniques. Once a broadband pulse is received, the pulse can be firstly truncated in the time domain to remove the non-line-of-sight signal. The magnitude spectrum of the pulse can be used to get an idea of where the signal is and the phase / time difference between the received signals at the two antennas can be applied to further improve the DF accuracy. Furthermore, the non-line-of-sight / reflected pulses also have magnitude and phase information that can help to learn the environment. Another example is the human auditory capability of learning the surrounding environment within seconds. It is interesting that blind people can judge distances of incoming sound sources. This capability can be studied to solve the multipath issue where the incident signal is unknown. Training or existing model is needed to build a database of the environment to apply this capability.

References

[1] S. E. Lipsky, *Microwave Passive Direction Finding*, John Wiley & Sons, Inc., New York, 1987.

[2] L.C. Godara, “Application of antenna arrays to mobile communications. II. Beam-forming and direction-of-arrival considerations,” *Proc. IEEE*, Vol. 85, no. 8, pp. 1195-1245, 1997.
[3] B. C. J. Moore, *Introduction to the Psychology of Hearing*, University Park Press, Baltimore, Maryland, 1977, pp. 169-208.
[4] E. Villchur, *Acoustics for Audiologists*, Singular Publishing Group, 2000.
[5] W. A. Yost, *Fundamentals of Hearing: An Introduction*, 4th ed., Academic Press, 2000.
[6] S. S. Stevens, and E. B. Newman, “The Localization of Actual Sources of Sound,” *Am. J. Psychol.*, Vol. 48, no. 2, pp. 297-306, 1936.
[7] T. T. Sandel, D. C. Teas, W. E. Feddersen, and L. A. Jeffress, “Localization of sound from single and paired sources,” *J. Acous. Soc. Am.*, vol. 27, issue: 9, pp. 842-852, 1955.
[8] L. A. Jeffress, “Detection and Lateralization of Binaural Signalsl,” *Audiology*, 10, pp. 77-84, 1971.
[9] H. Xin and J. Ding, “An improved two-antenna direction of arrival (DOA) technique inspired by human ears,” *IEEE AP-S Intl Symp. Dig.*, pp. 1-4, July. 2008.
[10] R. Zhou, H. Zhang and H. Xin, "Improved Two-Antenna Direction Finding Inspired by Human Ears," *IEEE Trans. Antennas Propag.*, July. 2011.
[11] R. A. Butler, “The monaural localization of tonal stimuli,” *Percept. Psychophys.*, vol. 9, pp. 99-101, 1971.
[12] J. Blauert, “Sound localization in median plane,” *Acoustica*, vol. 22, pp. 206-213, 1969.
[13] M. M. Van Wanrooij, Monaural adaptive mechanisms in human sound localization, Ph.D. dissertation, Dept. Biophysics, Radboud Univ., Nijmegen, Netherlands, 2007.
[14] J. Oppermann, M. Hamalainen, and J. Linatti, *UWB Theory and Applications*, John Wiley & Sons, Inc., 2004.
[15] H. Zhang, R. Zhou, Z. Wu, H. Xin, and R. W. Ziolkowski, “Designs of ultra wideband (UWB) printed elliptical monopole antennas with slots,” *Microw. Opt. Technol. Lett.*, vol. 52, pp. 466-471, 2010.
[16] R. Zhou and H. Xin, “A novel direction of arrival estimation technique using a single UWB antenna,” IEEE APSURSI Intl Symp., July, 2010
[17] G.M. Zelinski, G.A. Thiele, M.L. Hastriter, M.J. Havrilla and A.J. Terzuoli, “Half width leaky wave antennas,” *IET Microw. Antennas Propag.*, 2007, 1, (2), pp. 341–348.
[18] I. Getting, “The Global Positioning System,” *IEEE Spectrum*, vol. 30, no. 12, pp. 36-47, Dec. 1993.